

STRESS-RUPTURE AND STRESS-RELAXATION OF SiC/SiC COMPOSITES AT INTERMEDIATE TEMPERATURE

Gregory N. Morscher
Ohio Aerospace Institute
NASA Glenn Research Center, MS 106-5
Cleveland, OH 44135

Janet Hurst
NASA Glenn Research Center, MS 106-5
Cleveland, OH 44135

ABSTRACT

Tensile static stress and static strain experiments were performed on woven Sylramic® (Dow Corning, Midland, MI) and Hi-Nicalon™ (Nippon Carbon, Japan) fiber reinforced, BN interphase, melt-infiltrated SiC matrix composites at 815°C. Acoustic emission was used to monitor the damage accumulation during the test. The stress-rupture properties of Sylramic® composites were superior to that of Hi-Nicalon™ composites. Conversely, the applied strain levels that Hi-Nicalon™ composites can withstand for stress-relaxation experiments were superior to Sylramic® composites; however, at a cost of poor retained strength properties for Hi-Nicalon™ composites. Sylramic composites exhibited much less stress-oxidation induced matrix cracking compared to Hi-Nicalon™ composites. This was attributed to the greater stiffness and roughness of Sylramic® fibers themselves and the lack of a carbon layer between the fiber and the BN interphase for Sylramic® composites, which existed in Hi-Nicalon™ composites. Due to the lack of stress-relief for Sylramic composites, time to failure for Sylramic® composite stress-relaxation experiments was not much longer than for stress-rupture experiments when comparing the peak stress condition for stress-relaxation with the applied stress of stress-rupture.

INTRODUCTION

Woven SiC fiber reinforced composites utilizing a silicon-containing melt-infiltrated (MI) SiC matrix are candidate materials for a convectively cooled combustor liner application [1]. Use temperatures on the order of 1200°C are expected in the hottest regions of the combustor liner. However, the exterior of the combustor liner is expected to be at intermediate temperatures (less than 1000°C) and under tension due to thermal stresses. The stress condition is also expected to be more severe around areas of attachment between the combustor liner and the engine frame. This intermediate temperature, tensile stress condition poses a potential failure site of SiC/SiC composites for this application. Therefore, the time and environment dependent stress/strain properties of these materials at intermediate temperatures need to be understood and maximized.

The susceptibility to intermediate temperature embrittlement has been demonstrated by a number of researchers for SiC/SiC systems [2-6]. Interphases with better durability to oxygen and water vapor at intermediate temperatures result in superior stress rupture properties, i.e. BN interphases are superior to C interphases, and the more thermally stable fibers have improved intermediate temperature properties as well, i.e. Hi-Nicalon™ over Nicalon™ [4]. More thermally stable fibers are important for MI composites for two reasons: (1) the more thermally

This is a preprint or reprint of a paper intended for presentation at a conference. Because changes may be made before formal publication, this is made available with the understanding that it will not be cited or reproduced without the permission of the author.

stable fibers can withstand the MI process temperature with less degradation compared to less thermally stable fibers and (2) the strength of the fibers degrades less at intermediate temperature with time under stress-rupture conditions [7]. This as well as a number of other properties led to the selection of the Sylramic® fiber type as the fiber of choice for liner application of reference 1.

In this study, the intermediate temperature properties of the Sylramic® reinforced, BN interphase, MI SiC matrix composites will be compared with Hi-Nicalon™ reinforced, BN interphase, MI SiC matrix composites, specifically tensile stress-rupture and tensile stress-relaxation. Tensile stress-relaxation, though rarely studied, was sought after in this work because the actual combustor application is expected to be closer to a stress-relaxation condition rather than a stress-rupture condition.

EXPERIMENTAL

Static load stress-rupture tests were performed on Sylramic reinforced BN interphase, MI SiC composites (SYLMI) and static strain stress-relaxation experiments were performed on both SYLMI and Hi-Nicalon reinforced, BN interphase, MI SiC composites (HNMI). The composites were fabricated by Carborundum Corporation (Niagara Falls, NY) except for specimen SYLMIe (Table I) which was fabricated by Honeywell Advanced Composites (Newark, Delaware). The composites are made up of eight five-harness satin weave plies with an equal number of tows in the 0° and 90° directions (ends per inch). See reference 1 for processing details. Only a few specimens were made available from several different panels. Table I lists some of the pertinent physical properties of the specific specimens tested in this study.

An electromechanical driven Instron 4502 (Canton, Massachusetts) universal testing machine was used to perform both the stress-rupture and stress-relaxation experiments. Stress-rupture experiments were performed the same as described in reference 6. A capacitive mechanical extensometer was used to measure displacement for stress-rupture experiments and the extensometer was used in strain-control for the stress-relaxation tests. Stress and strain were measured for each test.

For a number of tests, AE activity was monitored (Fracture Wave Detector, Digital Wave Corp., Englewood, CO) as described in reference 6. Wide-band pass sensors were attached to the top and bottom edge of the 150 mm specimens inside the water-cooled grips. The sensors were physically in contact with the specimen and not the grip.

For some of the specimens, the fracture surface was examined with a field emission electron microscope (Hitachi S-4700, Tokyo, Japan) at 2 kV. For this setting, no conductive coating was required to examine the specimens. Specimens were also cut so that part of the length of the material that was in the hot zone could be polished longitudinally in order to measure the number and extent of matrix cracking into the thickness of the composite. After polishing, a plasma etch (400 kW in CF₄) was required in order to make the transverse matrix cracks visible in the SiC encasing the fibers in the load-bearing (0°) direction.

Table I: Properties of Specimens Tested

Specimen	Fiber Type / Ends Per Inch (epi)	Fiber Volume Fraction*	Elastic Modulus, GPa**	Type of Specimen
SYLMIa	Sylramic / 18 epi	0.18	270	Dogbone
SYLMIC	Sylramic / 18epi	0.17	222	Dogbone
SYLMId	Sylramic / 18 epi	0.18	269	Dogbone
SYLMIe	Sylramic / 22 epi	0.20	265	Straight-edge
HNMIb	Hi-Nicalon / 17epi	0.17	214	Straight-edge

* determined from epi, width of specimen, number of plies (8), number of fibers per tow (800 for Sylramic® and 500 for Hi-Nicalon™) and the average radius of the fibers (5 mm for Sylramic® and 6.5 mm for Hi-Nicalon™)

** linear regression fit of 0 to 50 MPa

RESULTS AND DISCUSSION

The room temperature stress-strain curves of the specimens tested in this study are shown in Figure 1. Also shown in Figure 1 are data from reference 1 (SYLMI[1]) and reference 6 (HNMIa). Essentially, for SYLMI composites, the “knee” in the stress-strain curves increases with volume fraction. However, there is some difference in the stress-strain curves for the different panels with the same volume fraction (HNMIa and HNMIb as well as SYLMIa and SYLMIb).

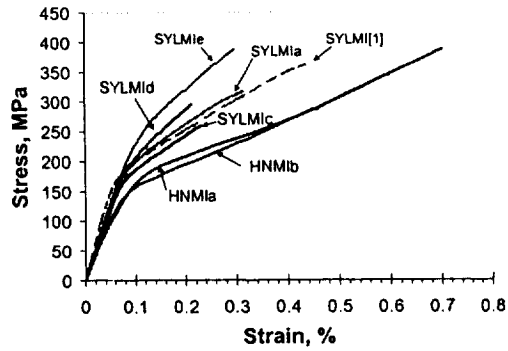
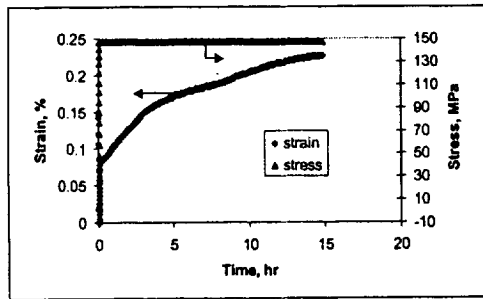
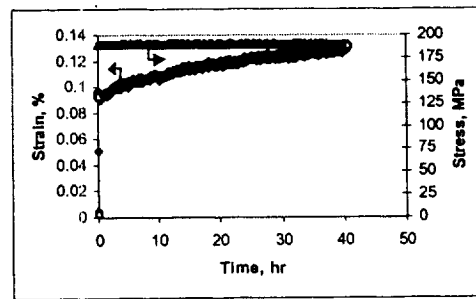


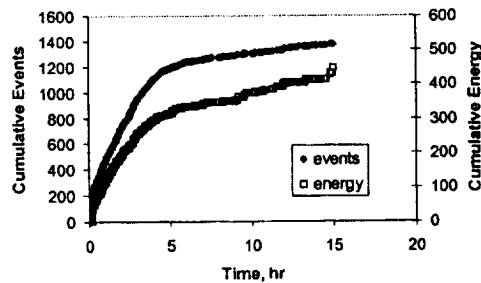
Figure 1: Room temperature tensile stress strain curves of different MI-SiC composites.



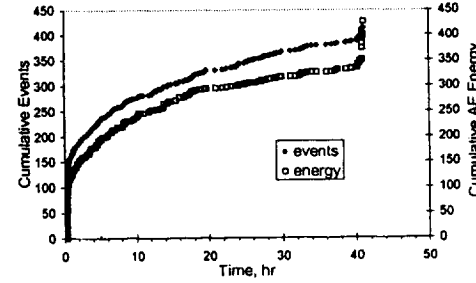
(a)



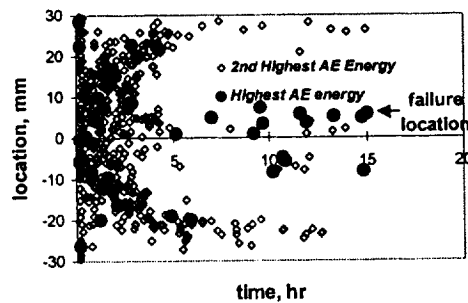
(a)



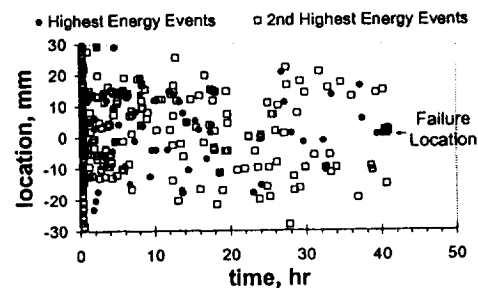
(b)



(b)



(c)



(c)

Figure 2: Mechanical and AE data for stress-rupture of a HNMIb specimen.

Figure 3: Mechanical and AE data for stress-rupture of a SYLMIb specimen.

For most of the stress-rupture and stress-relaxation tests, AE was monitored. Figures 2 and 3 show the stress-strain data, AE event and energy data, and location of AE events for a HNMIb specimen (reference 6) and a SYLMIa specimen from stress-rupture tests. Two differences were observed for the two composite systems in general. First, more AE activity occurred during the static-loading portion of the test for HNMI than for SYLMI, especially for longer time tests (> 10 hours). For HNMI composites, up to five times more AE energy was measured (e.g. the HNMIb specimen in Figure 2b) during static loading compared to the amount of AE energy measured during initial loading. This was indicative of a significant number of

matrix cracks that either formed or grew during the period of static loading [8]. The rapid crack growth in these composites was attributed to the presence of a carbon layer between the fiber and the BN interphase. The carbon layer most probably formed due to decomposition of the fiber during Si-infiltration [9] and was removed during the rupture test due to the oxidizing condition in the surface-exposed matrix cracks. For stresses at or below the "knee" stress (~ 155 MPa for HNMI, e.g. Figure 2), the removal of the carbon layer resulted in increased crack opening, which raised the stress intensity at the matrix crack tip and caused non-through-thickness microcracks to grow into and through the composite [8].

The SYLMI composites had much less AE activity during the static loading portion of the rupture experiments. The most AE activity recorded was for the specimen in Figure 3b. For that test, roughly the same amount of AE energy was recorded during the static portion as was recorded during initial loading. For most other SYLMI specimens, less than half the AE energy of that recorded during initial loading was recorded during the static portion of the experiment. Also, for the HNMI composite, most AE activity occurs in the first few hours whereas for the SYLMI composite, the amount of AE energy recorded decreases in rate with time more gradually. The propensity for crack growth in the HNMI composites, and the lack thereof for the SYLMI composites, was also reflected in the smaller amount of measured time-

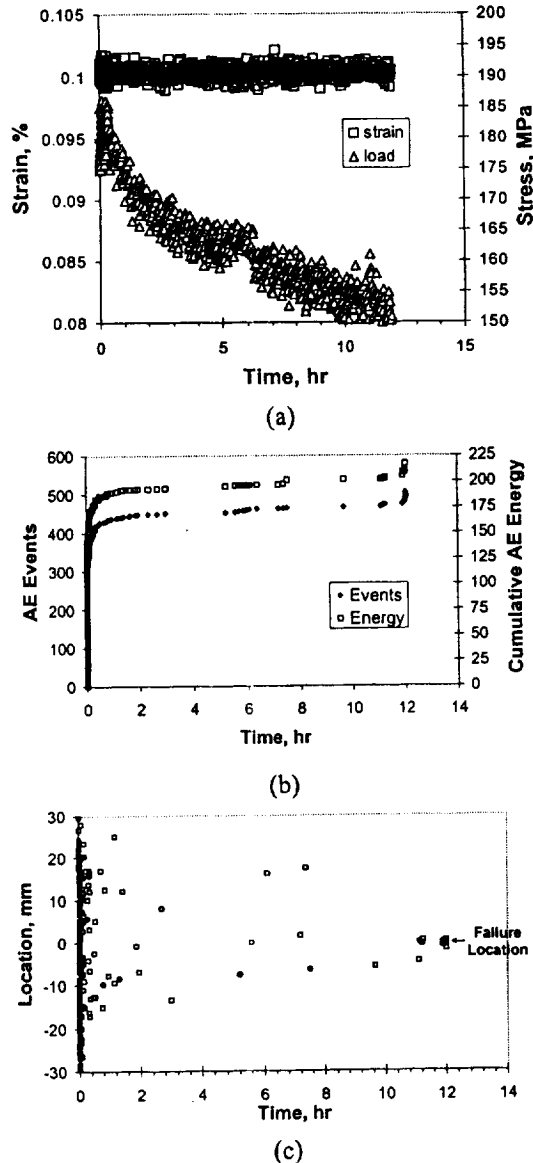


Figure 4: Mechanical and AE data recorded for a 0.1% SYLMIa stress-relaxation experiment.

dependent strain (see Figures 2a and 3a for HNMI and SYLMI, respectively)

Second, the events leading to ultimate composite failure appear to be different for longer time (> 10 hours) tests. Final failure for HNMI composites was usually characterized by a single loud event. Other events may have occurred in the region of final failure during the experiment well before final failure, but within a few minutes and usually hours of the failure time for a given specimen only the AE event corresponding to final failure occurred in the failure region (Figures 2b and c). For SYLMI composites, failure was characterized by several dozen events that occur within a few minutes time at the location of final failure (note the dramatic increase in AE events at failure in Figure 3b and the location of those events at the failure location in Figure 3c). This occurred for every SYLMI rupture test. Evidently, failure in SYLMI composites consisted of a number of progressive fiber and or matrix fracture events that lead to catastrophic failure, whereas HNMI composite failure was ultimately controlled by a single fracture event, presumably a fiber in an embrittled region of a matrix crack.

Figure 4 shows the stress-strain data, AE event-energy data, and location of AE events recorded during a stress-relaxation experiment. Note the high resolution of the stress/strain scale in Figure 4a. Minimal scatter in

the strain measurement was measured during the relaxation test and a relatively constant static strain level was maintained throughout the experiment. Less AE activity occurs during the static strain condition, which is to be expected given the stress relief that occurred. For SYLMI composites, failure was characterized by a number of events that occur in the failure location just prior to failure (Figure 4b and c) as was observed for rupture tests.

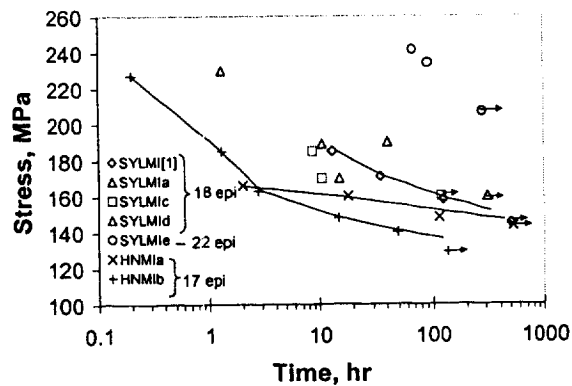


Figure 5: Stress-rupture of MI-SiC composites.

The stress-rupture data for the specimens tested in this study as well as for some data from reference 1 (SYLMI[1]) and reference 6 (HNMIa and HNMIb) are shown in Figure 5. Though only a few specimens were tested for each composite panel, it is evident that the intermediate temperature rupture stresses for a given panel follow the room temperature stress-strain behavior, i.e. panels with a higher "knee" stress require higher stresses to fail under intermediate temperature stress-rupture conditions. The "knee" in the stress-strain curve indicates where through-thickness cracking is prevalent. Since the oxidation embrittlement mechanisms controlling failure require access to the fibers and interphases [6], it is not surprising that rupture stresses correlate with stress-controlled damage in the matrix. The 22 epi SYLMIe composite performed the best, probably due to the highest "knee" stress as well as the highest volume fraction of fibers in the loading direction.

The stress-relaxation data for the specimens tested in this study are shown in Figure 6. For SYLMI composites, stress-relaxation was performed at a constant strain ranging from 0.08 to 0.15%. For HNMI composites, two experiments were performed, one at 0.2% and 0.25%. All of the SYLMI specimens (18 epi) tested for stress-relaxation failed whereas neither of the HNMIb specimens failed in the time allotted (140 hours).

Stress was relieved rapidly for HNMI composites compared to SYLMI composites. Within the first 10 hours, approximately 40% of the stress was relieved for the 0.2% stress-relaxation test (HNMI), most of that coming within the first hour. However, for the SYLMI

composites, only 5 to 20% of the stress was relieved in the first 10 hours and at a much slower rate than for HNMI composites.

The ultimate failure of Hi-Nicalon/BN/MI-SiC composites at intermediate temperatures depends on the oxidation kinetics causing fibers to strongly bond to one another or to the matrix followed by the failure of a single (or possibly a few) strongly bonded fibers. When a strongly bonded fiber fails, it causes the neighboring or possibly all the strongly bonded fibers in the crack to fail which results in the formation of a large unbridged crack that leads to catastrophic failure (see references 6 and 8). It appears that the stress-relief that occurs in HNMI composites was so great that even though all the fibers are bonded together, no fibers failed up to 140 hours. In reference 6, a specimen from the same HNMI panel was subjected to a static rupture condition of 129 MPa at 815°C and did not fail in 130 hours. Another specimen was precracked insuring a high crack density and then subjected to a static stress condition of 110 MPa at 815°C and did not fail in 130 hours. The "plateau" stresses (minimum) of the stress-relaxation test were ~ 115 MPa and 135 MPa for the 0.2% and 0.25% stress-relaxation tests, respectively, similar to the stress-rupture conditions where failure would not occur in reference 6. The fact that all the fibers are strongly bonded in the matrix crack was confirmed by the poor retained strength properties (below).

For the SYLMI composites, longitudinal sections of the hot zone section of one of the pieces of the tensile specimen were cut and polished in order to examine the amount of cracking and extent of crack propagation. The same approach was taken as in reference 8 where the number of cracks were counted in an outer ply and an inner ply and were averaged over a 10 mm length in order to get the average crack density. The crack density data for SYLMI and HNMIb composites [8] are plotted in Figure 7. Higher stresses are required to achieve similar crack densities for SYLMI composites compared to HNMIb. For the HNMIb specimens, the number of cracks in the outer plies was always greater than the number of cracks in the inner plies. This was because crack growth occurred from the microcracks that were exposed to the surface and grew into the composite, often linking up with cracks propagating from the opposite surface of the composite [8]. For the SYLMI composites, there were about twice as many interior cracks compared to the exterior cracks many of which do not extend to the free surface of the specimen. It was apparent that some crack opening occurred for surface cracks, but not to the extent that was

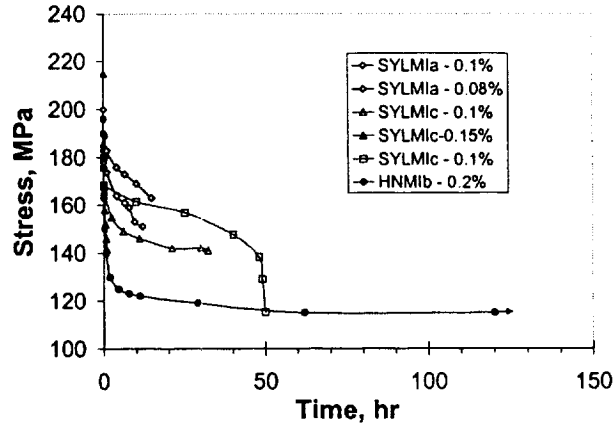


Figure 6: Stress-relaxation of MI-SiC composites.

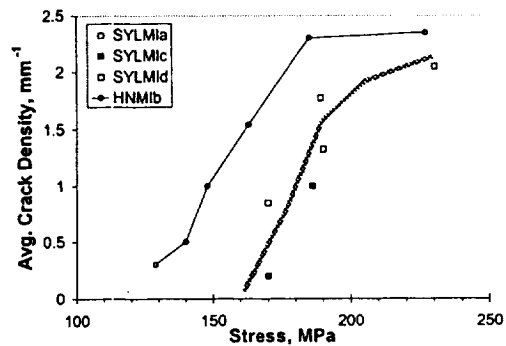


Figure 7: Average crack density for rupture specimens subjected to different static stress levels.

observed in reference 8. There are probably several reasons for this: the lack of a carbon layer between the Sylramic fiber and BN, a large interfacial shear strength (~ 70 MPa compared to ~ 25 MPa for Hi-Nicalon), and a high fiber modulus (380 GPa compared to 270 GPa for Hi-Nicalon) which all contribute to smaller crack openings.

The kinetics for oxygen ingress into a surface-exposed matrix crack could be determined from the fracture surfaces (not shown) by measuring the distance into the composite that the oxidation front reached. For HNMI composites this was rather straightforward because the unoxidized regions had large pullout lengths [6] and the demarcation between the oxidized (no pullout strongly bonded fibers) and unoxidized (large pullout) region was very clear. SYLMI composites have very short pullout lengths to begin with (0 to 10 μm) and a change in pullout length due to strong bonding is not so obvious. Therefore, the extent of oxidation from the edge of the fracture surface inwards was determined by the presence of oxidation at the fiber/matrix interphases using a field emission scanning electron microscope. Usually the oxidation region formed a "picture frame" [2] around the unembrittled region. Figure 8 shows the depth of oxidation into the specimen as a function of time at temperature. The kinetics for oxidation ingress of SYLMI composites are about half that of the HNMI composites.

One other critical property determined in this study was the retained strength of specimens that were subjected to the static stress or strain condition and did not fail during the stress-oxidation exposure. Several specimens from both SYLMI and HNMI composites were tested in tension at room temperature to failure after surviving stress-rupture or stress-relaxation testing (Figure 9). The retained strength of SYLMI specimens always exceeded the applied stress condition of the high temperature test whereas the retained strength of the HNMI specimens were always below the applied stress condition of the high temperature test. The better strength retention properties of SYLMI composites are presumably due to the greater resistance of these composites to crack growth of non-through thickness matrix cracks that are exposed to the environment in comparison to the HNMI composite.

Finally, one interesting observation is that for SYLMI composites, the time to failure for composite stress-relaxation is not much different than for composite stress-rupture, when the peak stress of the stress-relaxation condition is compared to the peak stress of the stress-rupture condition (Figure 10). It is difficult to model a changing stress condition; however, for the SYLMI composite system, it appears reasonable to use the results from a stress-rupture test as a criterion for optimized material down-selection.

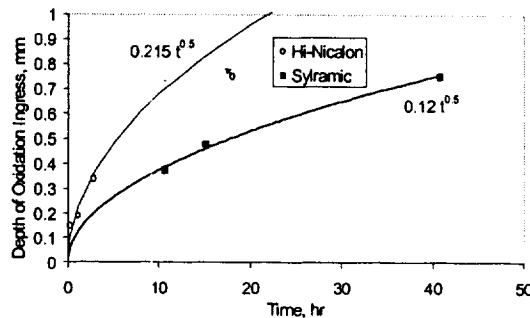


Figure 8: Depth of oxidation into the specimen from the surface of the composite versus rupture time for 815°C rupture. The specimen widths were 2 mm.

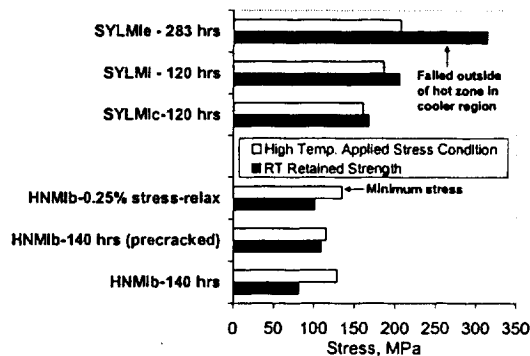


Figure 9: Retained strength of SYLMI and HNMI rupture and relaxation specimens that did not fail.

CONCLUSIONS

SYLMI was found to be superior to HNMI under static stress conditions, but HNMI was superior to SYLMI under static strain conditions at 815°C in air. The superior stress-rupture properties of SYLMI composites were attributed to the higher cracking stresses for these composites and the resistance to microcrack growth in these composites during the stressed-oxidation exposure. The ability of HNMI composites to relieve stress and survive large applied static strain conditions ($> 0.25\%$) was attributed to the oxidation of a carbon layer that exists between the fiber and BN interphase, i.e. due to a reduction in the interfacial shear stress and an increase in matrix crack opening. Unfortunately, this same mechanism leads to strong bonding between the fiber and matrix when the BN interphase is oxidized resulting in poor retained strength properties in comparison to SYLMI composites. For SYLMI composites, the time to failure for the stress-relaxation experiments was not that much different than the stress-rupture experiments when the peak stress of the stress-relaxation condition was compared with the applied stress of the stress-rupture condition. Therefore, the use of stress-rupture data as a criterion for constituent/architecture selection for a "constant strain" application such as a combustor liner appears appropriate for SYLMI composites.

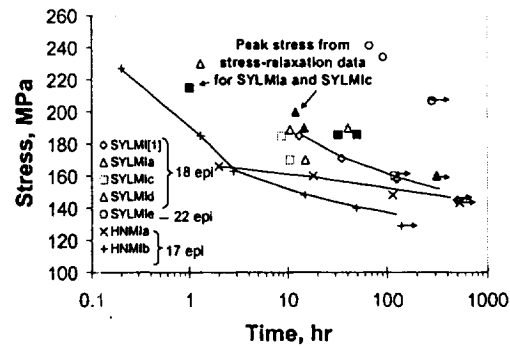


Figure 10: Peak Stress-relaxation data for SYLMI composites plotted on stress-rupture plot.

REFERENCES

1. D. Brewer, "HSR/EPM Combustor Materials Development Program," *Materials Science and Engineering A*, A261, 284-291 (1999)
2. F.E. Heredia, J.C. McNulty, F.W. Zok, and A.G. Evans, "Oxidation Embrittlement Probe for Ceramic-Matrix Composites," *Journal of the American Ceramic Society*, Vol. 78, No. 8, 1995, pp. 2097-2100.
3. P. Lipetzky, N.S. Stoloff, and G.J. Dvorak, "Atmospheric Effects on High-Temperature Lifetime of Ceramic Composites," *Ceramic Engineering Science Proceedings*, Vol. 18, No. 4, 1997, pp. 355-362.
4. G.N. Morscher, "Tensile Stress Rupture of SiC_f/SiC_m Minicomposites with Carbon and Boron Nitride Interphases at Elevated Temperatures in Air," *J. Am. Ceram. Soc.*, 80 [8] 2029-42 (1997)
5. Steyer, T.E. and Zok, F.W., "Stress Rupture of an Enhanced NicalonTM/SiC Composite at Intermediate Temperatures," *Journal of the American Ceramic Society*, Vol. 81, No. 8, 1998, pp. 2140-46
6. G.N. Morscher, J.H. Hurst, and D. Brewer, "Intermediate Temperature Stress Rupture of a Woven Hi-Nicalon, BN-Interphase, SiC Matrix Composite in Air," *Journal of the American Ceramic Society*, 83 [6] 1441-49 (2000)
7. H.M. Yun and J.A. DiCarlo, "Time/Temperature Dependent Tensile Strength of SiC and Al₂O₃-Based Fibers," pp. 17-26 in *Ceramic Transactions*, Vol. 74, *Advances in Ceramic-Matrix Composites III*. Eds. N. P. Bansal and J.P. Singh. American Ceramic Society, Westerville OH, 1996.
8. G.N. Morscher, "Growth of Matrix Cracks During Intermediate Temperature Stress Rupture of a SiC/SiC Composite in Air," *Ceram. Eng. Sci. Proc.*, 21 [3] 423-431 (2000)
9. L. U. J. T. Ogbuji, "Identification of a Carbon Sublayer in a Hi-Nicalon/BN/SiC Composite," *J. Mater. Sci. Letters*, vol. 18, pp. 1825-1827 (1999)